

Discrimination Reaction of O<sub>2</sub> and CO to 'Cross-strapped' Type Iron(II) Porphyrins

YOSHIO UEMORI and EISHIN KYUNO\*

School of Pharmacy, Hokuriku University, 3 Ho Kanagawa-Machi, Kanazawa 920-11 (Japan)

(Received April 28, 1989)

## Abstract

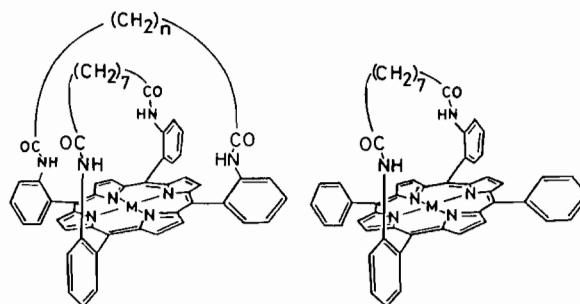
The syntheses and characterization of cross-strapped type iron(II) porphyrins with sterically protected cavities on one face are described. The porphyrins, in which one set of two amino groups in the *trans* position was bridged by heptamethylenedicarbonyl and the other by tetradecamethylenedicarbonyl or octadecamethylenedicarbonyl, were derived from the  $\alpha,\alpha,\alpha,\alpha$ -isomer of *meso*-tetra(*o*-aminophenyl)porphyrin. The heptamethylene chain was found to be crushed by the steric interaction with the tetradecamethylene chain bridged over the heptamethylene chain. The iron(II) complexes bind O<sub>2</sub> and CO reversibly in toluene containing 1,2-dimethylimidazole at 20 °C, and their O<sub>2</sub> and CO affinities have been determined. The O<sub>2</sub> and CO adducts of the iron(II) complexes have been characterized by <sup>1</sup>H NMR and IR spectra. The changes of the O<sub>2</sub> and CO affinities of the iron(II) complexes are discussed in terms of the polar effect of amide groups, the H-bonding of amide groups with O<sub>2</sub>, and the steric effects of cavities.

## Introduction

The proteins in hemoglobins and myoglobins play important roles in the discrimination reaction against the binding of CO relative to that of O<sub>2</sub>. The distal histidine (E7) is thought to be responsible for the reduced CO affinities, since the isolated  $\beta$  chain in HbZu\*\* ( $\beta_{63}\text{His} \rightarrow \text{Arg}$ ) has a high association rate

for CO binding and a high CO affinity [1]. The histidine can reduce CO affinity by steric and electronic effects. However, it is still unresolved which of the two effects is more important in lowering the CO affinity [2–9]. Furthermore, the studies have been designed and synthesized to fulfil the purpose of bridging the gap between the basic research conducted in the field of native hemoprotein and the simple model system thereof. From model complexes, many conflicting reports regarding the relative importance of these two effects on the discrimination have been given [10–14].

In order to address the steric role on the discrimination reaction in hemoproteins, a series of model porphyrins were designed and synthesized as shown in Fig. 1. We refer to the model porphyrins as 'cross-strapped' type porphyrins because one aliphatic chain overpasses another aliphatic chain bridging the same side of a porphyrin plane in these porphyrins. Here, each porphyrin has a cavity constructed by a so-called 'basket handle' and the size of cavity



$n = 14$  and  $18$ ;  $M = 2\text{H}, \text{Zn},$  and  $\text{Fe}$

Fig. 1. 'Cross-strapped' and 'strapped' porphyrins.

\* Author to whom correspondence should be addressed.

\*\* Abbreviations used: HbA, human adult hemoglobin; HbZu, hemoglobin Zurich; 1,2-Me<sub>2</sub>Im, 1,2-dimethylimidazole; 1-MeIm, 1-methylimidazole; 1,5-DCIm, 1,5-dicyclohexylimidazole; H<sub>2</sub>-Azam $\alpha\alpha$ , dianion of 5 $\alpha$ ,15 $\alpha$ -bis(2-amino-phenyl)-10 $\alpha$ ,20 $\alpha$ -(nonanediamidodi-*o*-phenylene)porphyrin; H<sub>2</sub>-Azam $\beta\beta$ , dianion of 5 $\beta$ ,15 $\beta$ -bis(2-amino-phenyl)-10 $\alpha$ ,20 $\alpha$ -(nonanediamidodi-*o*-phenylene)porphyrin; H<sub>2</sub>-Azampiv $\alpha\alpha$ , dianion of 5 $\alpha$ ,15 $\alpha$ -bis[2-(2,2-dimethylpropanamido)phenyl]-10 $\alpha$ ,20 $\alpha$ -(nonanediamidodi-*o*-phenylene)porphyrin; [Fe(piv<sub>2</sub>C<sub>8</sub>)], iron(II) complex of 5 $\alpha$ ,15 $\alpha$ -bis[2-(2,2-dimethylpropanamido)phenyl]-10 $\alpha$ ,20 $\alpha$ -(octanediamidodi-*o*-phenylene)porphyrin; [Fe(PPIDMe)], iron(II) complex of protoporphyrin

IX dimethyl ether; [Fe(PocPiv)], 5,10,15-(1,3,5-benzenetriacetyl)-20- $\alpha$ -*o*-pivalamidophenylporphyrinato iron(II); [Fe(MedPoc)], 5,10,15-(1,3,5-benzenetripropionyl)-20- $\alpha$ -*o*-pivalamidophenylporphyrinato iron(II); [Fe(piv<sub>2</sub>C<sub>9</sub>)], iron(II) complex of 5 $\alpha$ ,15 $\alpha$ -bis[2-(2,2-dimethylpropanamido)phenyl]-10 $\alpha$ ,20 $\alpha$ -(nonanediamidodi-*o*-phenylene)porphyrin;  $P_{1/2}$  (X), partial pressure of gaseous ligand (O<sub>2</sub>, CO) at half-saturation.  $M = P_{1/2}(\text{O}_2)/P_{1/2}(\text{CO})$ ; 'ruffling' refers to a distortion of the porphyrin ring toward  $D_{2d}$  geometry (see ref. 26).

can be varied by the changes in the length of aliphatic chain overpassing the basket handle. In this paper, we report the syntheses of the porphyrins, the O<sub>2</sub> and CO affinities of their Fe(II) complexes, and their IR and <sup>1</sup>H NMR data. The O<sub>2</sub> and CO binding to the porphyrins is discussed in terms of the polar effect of amide groups, the H-bonding of amide groups with O<sub>2</sub>, and the steric effects of cavities.

## Experimental

### General Information

Electronic spectra were recorded on a Hitachi 340 spectrophotometer. O<sub>2</sub> and CO affinities were determined by spectrophotometric titration using the flow method as described earlier [15]. The Fe(II) porphyrins were prepared by the mixing of Fe(III) porphyrins in toluene with aqueous sodium dithionite under Ar [13, 16]. Temperatures of the solutions were maintained at 25 ± 0.1 °C by the use of a constant-temperature circulation pump (Neslab Model RTE-8) and a variable-temperature cell holder (Hitachi). Various partial pressures of O<sub>2</sub> or CO were obtained by a gas mixture instrument (Kofloc Model GM-3A) constructed with mass flow controllers and flow meters. Concentrations of 1,2-Me<sub>2</sub>Im and Fe(II) porphyrins were 0.07 M and *c.* 1 × 10<sup>-5</sup> M, respectively. The spectra were recorded in the 500–350 nm range. *P*<sub>1/2</sub> values (half-saturation gas pressures for O<sub>2</sub> or CO binding) were calculated by the method of Beugelsdijk and Drago [17]. Reversibility was checked after the last CO or O<sub>2</sub> addition by purging with N<sub>2</sub> gas (7 ml/min) for 30 min; more than 90% reversibility was achieved after 2 h of carbonylation or oxygenation.

Proton NMR spectra were recorded on a JEOL GSX-400 spectrometer. Preparation of NMR samples were as follows. The Fe(III) porphyrin in CH<sub>2</sub>Cl<sub>2</sub> was reduced with aqueous sodium dithionite under Ar. After separation of the two phases, the dichloromethane layer was washed with degassed H<sub>2</sub>O and the solvent stripped off by passing Ar. The reduced product was then dissolved in degassed toluene-d<sup>8</sup> containing 1,2-Me<sub>2</sub>Im and transferred to 5 mm NMR tube via a stainless steel tube. The solution was then exposed to an atmosphere of O<sub>2</sub> or CO at room temperature. The spectra for the O<sub>2</sub> and CO adducts were obtained at -20 and 24 °C, respectively. The concentrations of the Fe(II) porphyrins and 1,2-Me<sub>2</sub>Im were *c.* 5 × 10<sup>-3</sup> M and 0.1 M, respectively.

Infrared spectra were obtained in benzene-d<sup>6</sup> with a CsI cell, using a JASCO DS-701G spectrometer. Samples were prepared in the same manner used for the preparations of <sup>1</sup>H NMR samples of CO adducts and recorded at room temperature.

The concentrations of Fe(II) porphyrins and 1,2-Me<sub>2</sub>Im were *c.* 5 × 10<sup>-3</sup> M and *c.* 0.1 M, respectively.

Mass spectra were obtained on a JEOL JMS-DX300 instrument.

### Materials

All solvents were of reagent grade, and used without further purification, except as noted below. Toluene was stirred with concentrated H<sub>2</sub>SO<sub>4</sub> and then washed with 5% NaOH and H<sub>2</sub>O, dried over CaCl<sub>2</sub>, and distilled. 1-MeIm and 1,2-Me<sub>2</sub>Im were vacuum distilled from KOH. Silica gel (Wakogel C-200) was used for column chromatography. The 8.97% O<sub>2</sub> in N<sub>2</sub> mixture and the 995 ppm CO in N<sub>2</sub> mixture were commercially purchased.

### Synthesis

5,15-diphenyl-10α,20α-bis(nonanediamidodi-*o*-phenylene)porphyrin (H<sub>2</sub>-AzP) and its iron(III) complexes were prepared by the method described before [15, 18]. The acid chlorides were prepared by treating the appropriate acids with thionyl chloride [11c]. 1,5-DCIm was prepared according to the literature [14d].

#### *5α,15α-bis(nonanediamidodi-*o*-phenylene)-10α,20α-bis(eicosanediamidodi-*o*-phenylene)porphyrin (H<sub>2</sub>-AzC18α)*

A CH<sub>2</sub>Cl<sub>2</sub> solution (400 ml) of H<sub>2</sub>-Azamα [15] (300 mg, 0.363 mmol) was treated with pyridine (0.5 ml) and eicosanedioyl dichloride (0.3 g, 0.8 mmol) at room temperature. The solution was stirred for 1 h, then 10% aqueous ammonia (100 ml) was added, and the solution was stirred for 0.5 h. The organic layer was separated and evaporated to dryness. The resultant solid was dissolved in CHCl<sub>3</sub> and chromatographed on a silica gel column (CHCl<sub>3</sub>, 4 × 30 cm). The column was eluted with CHCl<sub>3</sub>/ether (9:1). The product was recrystallized from benzene hexane, yielding 210 mg (52%). *Anal.* Calc. for C<sub>73</sub>H<sub>80</sub>N<sub>8</sub>O<sub>4</sub>: C, 77.35; H, 7.11; N, 9.89. Found: C, 77.21; H, 6.96; N, 9.61%. FAB-MS: *m/e* 1133 (*M*<sup>+</sup> + 1). <sup>1</sup>H NMR data are shown in Table 1.

#### *5α,15α-bis(nonanediamidodi-*o*-phenylene)-10α,20α-bis(hexadecanediamidodi-*o*-phenylene)porphyrin (H<sub>2</sub>-AzC14α)*

This was prepared from H<sub>2</sub>-Azamα (200 mg, 0.242 mmol) in the same manner as H<sub>2</sub>-AzC18α, except hexadecanedioyl dichloride (0.3 g, 0.9 mmol) in place of eicosanedioyl dichloride was used, yielding 160 mg (61%). *Anal.* Calc. for C<sub>69</sub>H<sub>72</sub>N<sub>8</sub>O<sub>4</sub>: C, 76.92; H, 6.74; N, 10.40. Found: C, 76.53; H, 6.64; N, 9.79%. FAB-MS: *m/e* 1077 (*M*<sup>+</sup> + 1). <sup>1</sup>H NMR data are shown in Table 1.

TABLE 1. <sup>1</sup>H NMR data

|   | Protons of the C7-chain <sup>a</sup> |       |       |       | Amide  | Protons      | Remarks |
|---|--------------------------------------|-------|-------|-------|--------|--------------|---------|
|   | α                                    | β     | γ     | δ     |        |              |         |
| H <sub>2</sub> -AzP                                   | +1.16                                | -1.22 | -0.50 | -2.50 |        | +6.00        | b, h    |
| [Zn(AzP)]   | +1.17                                | -1.36 | -0.50 | -2.65 |        | +6.05        | b       |
| [Zn(AzP)(1,2-Me <sub>2</sub> Im)]                     | +1.11                                | -1.29 | -0.55 | -2.63 |        | +6.06        | c       |
| [Fe(AzP)(1,2-Me <sub>2</sub> Im)(CO)]                 | +0.57                                | +0.57 | +0.11 | -1.02 |        | +5.83        | d, h    |
| [Fe(AzP)(1,2-Me <sub>2</sub> Im)(O <sub>2</sub> )]    | +1.28                                | +0.95 | +0.17 | -0.98 | +7.96  | +4.56        | e, h    |
| H <sub>2</sub> -AzC14α                                | +1.21                                | -1.67 | -1.50 | -3.79 | +6.72, | +6.42        | b       |
| [Zn(AzC14α)]  | +1.11                                | -1.84 | -1.46 | -3.84 | +6.65  | +6.39        | b       |
| [Zn(AzC14α)(1,2-Me <sub>2</sub> Im)]                  | +1.21                                | -1.87 | -1.39 | -4.12 | +6.75  | +6.46        | c       |
| [Fe(AzC14α)(1,2-Me <sub>2</sub> Im)(CO)]              | +1.20                                | -0.44 | -0.02 | -1.38 | +6.90  | +6.29        | d       |
| [Fe(AzC14α)(1,2-Me <sub>2</sub> Im)IO <sub>2</sub> ]  | +1.09                                | -0.67 | -0.16 | -1.39 | +8.25  | +5.67, +4.59 | e       |
| H <sub>2</sub> -AzC18β                                | +1.17                                | -1.32 | -0.55 | -2.60 | +6.71  | +6.00        | b       |
| H <sub>2</sub> -AzC18α                                | +1.21                                | -1.47 | -1.17 | -3.11 | +7.12  | +6.34        | b       |
| [Zn(AzC18α)]  | +1.14                                | -1.65 | -1.16 | -3.27 | +6.98  | +6.30        | b       |
| [Zn(AzC18α)(1,2-Me <sub>2</sub> Im)]                  | +1.21                                | -1.72 | -1.17 | -3.54 | +7.01  | +6.37        | c       |
| [Fe(AzC18α)(1,2-Me <sub>2</sub> Im)(CO)]              | +0.86                                | +0.58 | +0.34 | -0.50 | +7.01  | +5.84        | d       |
| [Fe(AzC18α)(1,2-Me <sub>2</sub> Im)(O <sub>2</sub> )] | f                                    | f     | +0.39 | -0.42 | +7.73  | g, +4.62     | e       |

<sup>a</sup>The letters (α-δ) refer to -NHCO-CH<sub>2</sub>CH<sub>2</sub>CH<sub>2</sub>CH<sub>2</sub>CH<sub>2</sub>CH<sub>2</sub>CH<sub>2</sub>-CONH-. <sup>b</sup>Solvent = CDCl<sub>3</sub>. <sup>c</sup>Solvent = CDCl<sub>3</sub> containing 1,2-dimethylimidazole (0.1 M). <sup>d</sup>Solvent = toluene-d<sub>8</sub> containing 1,2-dimethylimidazole (0.1 M). <sup>e</sup>Solvent was the same in d, measured at -20 °C. <sup>f</sup>Resonances were obscured by the signals of the C18-chain (+0.82 to 1.61 ppm). <sup>g</sup>Resonance was obscured by either the signals of 1,2-dimethylimidazole (6.25-6.4 and 7.1-7.25 ppm) or those of undeuterated toluene (6.9-7.1 and 7.1-7.2 ppm). <sup>h</sup>Ref. 18.

*5α,15α-bis(nonanediamidodi-o-phenylene)-10β,20β-bis(eicosanediamidodi-o-phenylene)-porphyrin (H<sub>2</sub>-AzC18β)*

This was prepared from H<sub>2</sub>-Azamββ [19] (150 mg, 0.182 mmol) in the same manner as H<sub>2</sub>-AzC18α, yielding 100 mg (49%). *Anal.* Calc. for C<sub>73</sub>H<sub>80</sub>N<sub>8</sub>O<sub>4</sub>; C, 77.35; H, 7.11; N, 9.89. Found: C, 76.74; H, 7.15; N, 9.81%. FAB-MS: *m/e* 1133 (*M*<sup>+</sup> + 1). <sup>1</sup>H NMR data are shown in Table 1.

*Fe(III) insertion*

Iron(III) complexes were prepared by heating the porphyrins with FeBr<sub>2</sub> in acetic acid containing 2% sodium acetate (wt./wt.) at 70 °C [20]. Purification was carried out on a silica gel column using CHCl<sub>3</sub>/CH<sub>3</sub>OH (95:5) as the eluent. The product was evaporated to dryness and then treated with concentrated HBr in CHCl<sub>3</sub>. After being dried over Na<sub>2</sub>SO<sub>4</sub>, the solvent was reduced in volume on a rotary evaporator and the product was precipitated by adding hexane.

[Fe(AzC18α)]Br. *Anal.* Calc. for C<sub>73</sub>H<sub>78</sub>N<sub>8</sub>O<sub>4</sub>-FeBr·CHCl<sub>3</sub>: C, 64.10; H, 5.74; N, 8.08. Found: C, 64.38; H, 6.04; N, 8.03%. UV-Vis λ<sub>max</sub> (CHCl<sub>3</sub>): 420 nm (log ε 4.93), 515 (4.13), 584 (3.51), 664 (3.45), 690 (3.48).

[Fe(AzC14α)]Br. *Anal.* Calc. for C<sub>69</sub>H<sub>70</sub>N<sub>8</sub>O<sub>4</sub>-FeBr·CHCl<sub>3</sub>: C, 63.19; H, 5.38; N, 8.42. Found:

C, 63.30; H, 5.47; N, 8.74%. UV-Vis λ<sub>max</sub> (CHCl<sub>3</sub>): 419 nm (log ε 4.95), 510 (4.16), 580 (3.56), 652 (3.53), 680 (3.47).

*Zn(II) insertion*

Zn(II) complexes were prepared by heating the porphyrins with Zn(CH<sub>3</sub>COO)<sub>2</sub>·2H<sub>2</sub>O in acetic acid at 70 °C. The reaction mixture was then evaporated to dryness. The residue was dissolved in CHCl<sub>3</sub> and washed with 10% NaOH/H<sub>2</sub>O. After being dried over Na<sub>2</sub>SO<sub>4</sub>, the solution was evaporated to dryness and the product was crystallized from hot methanol.

[Zn(AzP)]. *Anal.* Calc. for C<sub>53</sub>H<sub>42</sub>N<sub>6</sub>O<sub>2</sub>Zn·CH<sub>3</sub>OH·½CHCl<sub>3</sub>: C, 68.76; H, 4.92; N, 8.83. Found: C, 68.62; H, 4.70; N, 8.73%.

[Zn(AzC18α)]. *Anal.* Calc. for C<sub>73</sub>H<sub>78</sub>N<sub>8</sub>O<sub>4</sub>Zn·H<sub>2</sub>O: C, 72.17; H, 6.64; N, 9.22. Found: C, 72.00; H, 6.75; N, 9.10%.

[Zn(AzC14α)]. *Anal.* Calc. for C<sub>69</sub>H<sub>70</sub>N<sub>8</sub>O<sub>4</sub>Zn: C, 72.65; H, 6.19; N, 9.82. Found: C, 72.09; H, 6.24; N, 9.74%.

**Results**

*Synthesis*

The treatment of H<sub>2</sub>-Azamαα with approximately two molar equivalents of ClCO(CH<sub>2</sub>)<sub>n</sub>COCl (*n* = 14

and 18) gave H<sub>2</sub>-AzC14 $\alpha$  and H<sub>2</sub>-AzC18 $\alpha$ , respectively. For the aid of characterization, the atropisomer of H<sub>2</sub>-AzC18 $\alpha$  was prepared from the reaction of H<sub>2</sub>-Azam $\beta\beta$  with ClCO(CH<sub>2</sub>)<sub>18</sub>COCl. The yields of H<sub>2</sub>-AzC14 $\alpha$  and H<sub>2</sub>-AzC18 $\alpha$  were 61% and 52%, respectively. The porphyrins were characterized by <sup>1</sup>H NMR, mass spectroscopy and elemental analysis.

Because of C<sub>2v</sub> symmetry for both H<sub>2</sub>-AzC14 $\alpha$  and H<sub>2</sub>-AzC18 $\alpha$ , and D<sub>2h</sub> symmetry for H<sub>2</sub>-AzC18 $\beta$ , these porphyrins show four separated signals for the protons of the C7-chains in the <sup>1</sup>H NMR spectra. Each signal could be assigned on the basis of spin-decoupling experiments and their relative intensities (Table 1). The  $\beta$  proton signals appeared at higher magnetic fields than the  $\gamma$  proton signals. The  $\delta$  proton signal of each H<sub>2</sub>-AzC14 $\alpha$  and H<sub>2</sub>-AzC18 $\alpha$  was shifted to higher magnetic field by 1.29 and 0.61 ppm, respectively, compared with that of H<sub>2</sub>-AzP. The  $\gamma$  and  $\beta$  proton signals of H<sub>2</sub>-AzC14 $\alpha$  also appeared at higher fields than those of H<sub>2</sub>-AzC18 $\beta$  and H<sub>2</sub>-AzP, while the  $\alpha$  proton signals appeared to be nearly constant among the porphyrins prepared. The signals of the C14-chain and the C18-chain overlapped, and therefore could not be assigned well.

The iron(III) complexes were prepared from the porphyrins by the acetate method [20]. The reaction temperatures were kept below 70 °C to prevent the atropisomerization of phenyl rings. Such isomerization was not observed for the case of H<sub>2</sub>-AzC14 $\alpha$  even in refluxing toluene for 3 h, while 10% of H<sub>2</sub>-AzC18 $\alpha$  was found to isomerize into H<sub>2</sub>-AzC18 $\beta$  under these conditions. The lack of isomerization during iron insertion was confirmed by the <sup>1</sup>H NMR spectra of the CO adducts.

#### O<sub>2</sub> and CO Affinities

The O<sub>2</sub> and CO affinities for the iron(II) porphyrins were determined spectrophotometrically in toluene containing 1,2-Me<sub>2</sub>Im as the axial base. The spectral changes upon O<sub>2</sub> and CO titrations are shown in Figs. 2 and 3, respectively. The P<sub>1/2</sub>(O<sub>2</sub>) value for [Fe(AzC14 $\alpha$ )(1,2-Me<sub>2</sub>Im)] was extrapolated from the van't Hoff plots. The following data used in the van't Hoff plots. The following data used in the van't Hoff plots, represent the pairs of temperature (°C) and P<sub>1/2</sub>(O<sub>2</sub>) (torr): (11, 893), (5.4, 667), (0, 283), (-9.1, 127), (-15.7, 58), and (-22.4, 28). Table 2 lists the data of O<sub>2</sub> and CO affinities, together with that of related complexes. The solvent dependence of O<sub>2</sub> affinities for [Fe(AzC14 $\alpha$ )] was also examined at 0 °C with 1,2-Me<sub>2</sub>Im as an axial base. The P<sub>1/2</sub>(O<sub>2</sub>) values for [Fe(AzC14 $\alpha$ )] in mesitylene, toluene and *o*-dichlorobenzene were 260, 283 and 362 torr, respectively.

#### <sup>1</sup>H NMR Spectra for the O<sub>2</sub> and CO Adducts

To determine the structural details of the O<sub>2</sub> and CO adducts, <sup>1</sup>H NMR spectra were measured

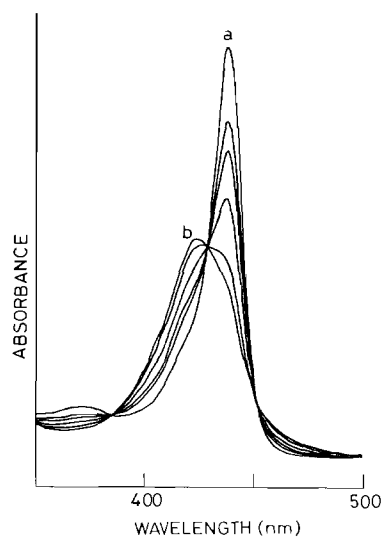


Fig. 2. Spectral changes upon addition of O<sub>2</sub> to [Fe(AzC14- $\alpha$ )], *c.* 1  $\times$  10<sup>-5</sup> M in toluene, 0.07 M in 1,2-Me<sub>2</sub>Im, -9.1 °C: curve (a) under N<sub>2</sub>; curve (b) under 760 Torr of O<sub>2</sub>. The following partial pressures of O<sub>2</sub> were used: 43, 76, 152 and 380 Torr.

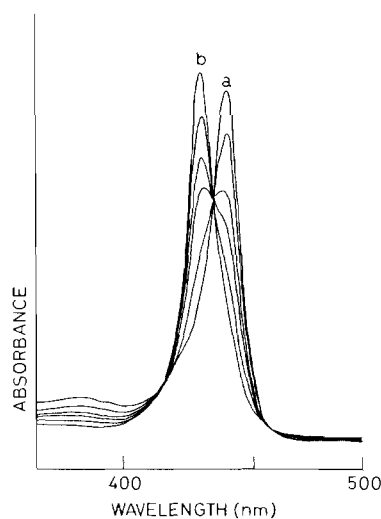


Fig. 3. Spectral changes upon addition of CO to [Fe(AzC14 $\alpha$ )], *c.* 1  $\times$  10<sup>-5</sup> M in toluene, 0.07 M in 1,2-Me<sub>2</sub>Im, 20 °C: curve (a) under N<sub>2</sub>; curve (b) under 393 Torr of CO. The following partial pressures of CO were used: 16, 46, 81 and 160 Torr.

in toluene-d<sup>8</sup> solution containing Fe(II) porphyrins (*c.* 5 mM) and 1,2-Me<sub>2</sub>Im (*c.* 0.1 M), and are shown in Figs. 4 and 5, and Table 1. The spectra were recorded at -20 °C for the O<sub>2</sub> adducts to minimize the influence of five coordinate species. The <sup>1</sup>H NMR spectra of both Zn(II) complexes and their 1,2-Me<sub>2</sub>Im adducts were virtually identical with those of the corresponding free base porphyrins. Contrary to this, the chemical shifts of C7-chain protons in the O<sub>2</sub> and CO adducts were significantly

TABLE 2. O<sub>2</sub> and CO binding to iron(II) porphyrins

| Complexes                 | $P_{1/2}(\text{O}_2)$ (Torr) | $P_{1/2}(\text{CO})$ (Torr) | $M^a$ | Conditions | References |
|---------------------------|------------------------------|-----------------------------|-------|------------|------------|
| [Fe(AzP)]                 | 18                           | 0.05                        | 360   | b          | this work  |
| [Fe(AzC14 $\alpha$ )]     | 2150                         | 62                          | 35    | b          | this work  |
| [Fe(AzC14 $\alpha$ )]     | 18                           | 0.31                        | 58    | c          | this work  |
| [Fe(AzC18 $\alpha$ )]     | 15                           | 0.09                        | 170   | b          | this work  |
| [Fe(PocPiv)]              | 12.6                         | 0.067                       | 216   | d          | 11d        |
| [Fe(MedPoc)]              | 12.4                         | 0.026                       | 480   | d          | 11d        |
| [Fe(piv <sub>2</sub> C8)] | 0.1                          | 0.011                       | 7     | e          | 13         |
| [Fe(piv <sub>2</sub> C9)] | 0.033                        | 0.00028                     | 89    | e          | 13         |
| 5,5-Pyridine              | 540                          | 37                          | 14    | f          | 14e        |
| Cyclophaneheme            |                              |                             |       |            |            |

<sup>a</sup> $M = P_{1/2}(\text{O}_2)/P_{1/2}(\text{CO})$ . <sup>b</sup>At 20 °C in toluene, 0.07 M in [1,2-dimethylimidazole (1,2-Me<sub>2</sub>Im)]. <sup>c</sup>At 20 °C in toluene, 0.07 M in [1,5-dicyclohexylimidazole (1,5-DCIm)]. <sup>d</sup>At 25 °C in toluene, 0.1 M in [1,2-Me<sub>2</sub>Im]. <sup>e</sup>At 20 °C in toluene, 0.01 M in [1-methylimidazole]. <sup>f</sup>At 20 °C in toluene, 0.7 M in [1,5-DCIm].

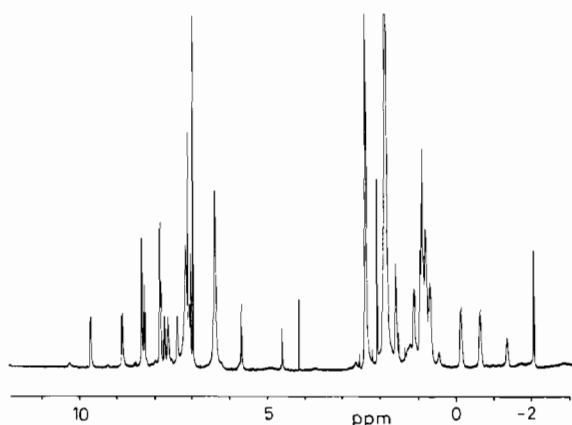


Fig. 4. <sup>1</sup>H NMR spectrum of the O<sub>2</sub> adducts of [Fe(AzC14 $\alpha$ )], *c.*  $5 \times 10^{-3}$  M in toluene-d<sup>8</sup> containing 1,2-Me<sub>2</sub>Im (0.1 M) at -20 °C.

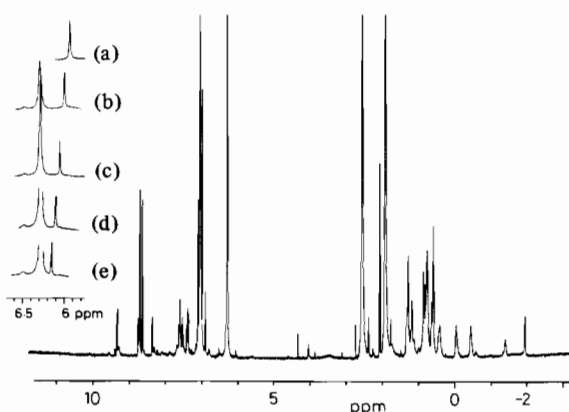


Fig. 5. <sup>1</sup>H NMR spectrum of the CO adducts of [Fe(AzC14 $\alpha$ )], *c.*  $5 \times 10^{-3}$  M in toluene-d<sup>8</sup> containing 1,2-Me<sub>2</sub>Im (0.1 M) at 24 °C. Insert: The shifts of the amide proton signals upon addition of 1,2-dimethylimidazole (1,2-Me<sub>2</sub>Im); [Fe(AzC14 $\alpha$ )] = 4.5 mM. Concentration of 1,2-Me<sub>2</sub>Im are (a), 9; (b), 26; (c), 43; (d), 61; (e), 78 mM. The peak at 6.3 ppm is due to excess 1,2-Me<sub>2</sub>Im.

TABLE 3. CO stretching frequencies

|                       | $\nu(\text{CO})$ (cm <sup>-1</sup> )                      | References |
|-----------------------|---|------------|
| [Fe(AzP)]             | 1960 <sup>a</sup> , 1955 <sup>b</sup>                     | this work  |
| [Fe(AzC14 $\alpha$ )] | 1948 <sup>a</sup> , 1945 <sup>b</sup>                     | this work  |
| [Fe(AzC18 $\alpha$ )] | 1951 <sup>a</sup> , 1948 <sup>b</sup>                     | this work  |
| HbA                   | 1951 <sup>c</sup>   | 21         |
| [Fe(PPIXDMe)]         | 1980 <sup>d</sup> , 1969 <sup>e</sup> , 1959 <sup>f</sup> | 21         |

<sup>a</sup>Solvents are benzene-d<sup>6</sup>, 0.1 M in [1-methylimidazole(1-MeIm)]. <sup>b</sup>Solvents are benzene-d<sup>6</sup>, 0.1 M in [1,2-dimethylimidazole]. <sup>c</sup>Aqueous media. <sup>d</sup>Solvents are 1-MeIm in CCl<sub>4</sub>. <sup>e</sup>Solvents are 1-MeIm in CHCl<sub>3</sub>. <sup>f</sup>Solvents are 1-MeIm in ClCH<sub>2</sub>-CH<sub>2</sub>Cl.

different from those of the corresponding free base porphyrins.

#### IR Spectra for the CO Adducts

Table 3 lists CO stretching frequencies. In [Fe(AzC18 $\alpha$ )(1,2-Me<sub>2</sub>Im)(CO)], the CO stretching frequency was independent of 1,2-Me<sub>2</sub>Im concentration when between approximately 2 and 400 molar equivalents of the base were used. The  $\nu(\text{CO})$  value of [Fe(AzC14 $\alpha$ )(1,2-Me<sub>2</sub>Im)(CO)] was found to increase by 2 cm<sup>-1</sup>, while that of [Fe(AzP)(1,2-Me<sub>2</sub>Im)(CO)] was found to decrease by 2 cm<sup>-1</sup> upon addition of 1,2-Me<sub>2</sub>Im.

#### Discussion

##### Synthesis

Considering their structures, the tetradecamethylene (C14-chain) or octadecamethylene (C18-chain) chain must bridge 'over' the heptamethylene chain (C7-chain) in the  $\alpha$  isomers, it is interesting that the yield of these porphyrins is comparable to that of H<sub>2</sub>-AzC18 $\beta$ .

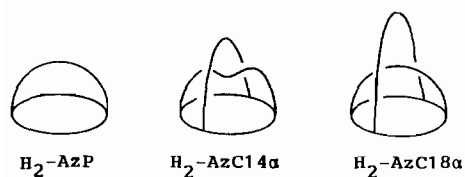


Fig. 6. Schematic representation of the strapping chains. The ovals represent porphyrin planes and the loops represent the strapping chains.

The influence of ring current of a porphyrin increases in strength both approaching the porphyrin plane and the ligand axis through the metal [22]. The high field shifts of resonances for the C7-chain protons in  $H_2$ -AzC18 $\alpha$  are mainly due to the prevention of lateral movement of the C7-chain, because these values are comparable to those of  $H_2$ -Azpiv $\alpha$  [13, 15] in which the C7-chain is considered to lie just above the porphyrin center by the steric interaction with two pivalamido groups [23]. According to CPK models, the C7-chain in  $H_2$ -AzC18 $\alpha$  lies approximately 2.8 Å below the C18-chain, while that of  $H_2$ -AzC14 $\alpha$  lies in contact with a C14-chain. In addition to the shift of the  $\delta$  protons to the higher magnetic field, the chemical shift value of the  $\gamma$  protons in  $H_2$ -AzC14 $\alpha$  approaches the values of the  $\beta$  protons. This means that both the  $\delta$  and  $\gamma$  protons are pushed down to the porphyrin plane. Thus, it is reasonable to expect that the C7-chain is crushed by the steric repulsion with the C14-chain as shown in Fig. 6. Therefore, the shifts of the C7-chain proton signals in  $[Fe(AzC14\alpha)(1,2-Me_2Im)(CO)]$  are concluded to be the result of the crushing of the C7-chain.

#### $^1H$ NMR Spectra for the $O_2$ and CO Adducts

The  $\delta$  proton signals of  $[Fe(AzP)(1,2-Me_2Im)(CO)]$  appear at higher magnetic field than those of  $[Fe(AzC18\alpha)(1,2-Me_2Im)(CO)]$ . This may result from the lateral movement of the C7-chain in  $[Fe(AzP)(1,2-Me_2Im)(CO)]$ . By this movement, the  $\delta$  protons suffer less shielding of the ring current by the bound CO molecule than the others. In addition to the case of the free base porphyrins, the factors affecting the chemical shifts of the C7-chain protons in the CO adducts are considered to be both the shielding of the porphyrin ring current by CO and magnetic anisotropy of CO. Furthermore, it is difficult to evaluate the two effects separately in the present study. Thus, further discussion on the interaction of the C7-chain with CO using  $^1H$  NMR data will be impossible. Increasing the concentration of 1,2- $Me_2Im$ , the amide proton signals of the C7-chain in  $[Fe(AzC14\alpha)(1,2-Me_2Im)(CO)]$  shift from 5.95 to 6.25 ppm, as shown in Fig. 5. Such shift of the amide proton signals is not observed for the other two complexes. Therefore, these observations imply

that the amide protons of the C7-chain in  $[Fe(AzC14\alpha)(1,2-Me_2Im)(CO)]$  are directed to the position where the amide protons receive the interaction with the excess 1,2- $Me_2Im$  added.

The C7-chain resonances for the  $O_2$  adducts also differ from each other, as in the case of the CO adducts. The amide proton signals in  $[Fe(AzC14\alpha)(1,2-Me_2Im)(O_2)]$  appear at 8.25, 5.67 and 4.59 ppm (relative intensity was 1:2:1). The split of the amide proton signals at 8.25 and 4.59 ppm is due to H-bonding with  $O_2$  [24, 18]. On the other hand, the signals of the amide protons forming the H-bonding with  $O_2$  in  $[Fe(AzC18\alpha)(1,2-Me_2Im)(O_2)]$  appear at 7.73 and 4.65 ppm, but any other amide proton signal was obscured by the resonances due to 1,2- $Me_2Im$  or undeuterated toluene. The amide proton signals of the C14-chain and the C18-chain appear at similar positions in the CO adducts and the Zn(II) complexes. Thus, the signal at 5.67 ppm in the spectrum for  $[Fe(AzC14\alpha)(1,2-Me_2Im)(O_2)]$  is assigned to the amide protons of the C7-chain: if that signal is due to the amide protons of the C14-chain, the amide proton signal of the C18-chain in  $[Fe(AzC18\alpha)(1,2-Me_2Im)(O_2)]$  must appear near 5.6 ppm, however, such a signal was not observed near 5.6 ppm. Therefore, it is concluded that the amide groups forming H-bonding with the bound  $O_2$  molecules are not of the C7-chain, but of the C14-chain. The conformational changes in the amide groups might be due to the influence of the crushing in the C7-chain. On the other hand, the amide protons forming the H-bonding in  $[Fe(AzC18\alpha)(1,2-Me_2Im)(O_2)]$  are the same as in the case of  $[Fe(AzP)(1,2-Me_2Im)(O_2)]$  [18]. The  $\beta$  and  $\gamma$  proton signals of the C7-chain in  $[Fe(AzC14\alpha)(1,2-Me_2Im)(O_2)]$  are shifted to higher magnetic fields compared with the corresponding CO adducts. Such shifts are not observed in the other two complexes; therefore, these may be responsible for the differences in the interactions of  $O_2$  or CO with the C7-chain.

#### IR Spectra for the CO Adducts

The solvent dependences of  $\nu(CO)$  for the CO adducts are small compared to those observed by Maxwell and Caughy [21] (*c.* 20  $cm^{-1}$ ); the reduction of  $\nu(CO)$  for  $[Fe(AzP)(1,2-Me_2Im)(CO)]$  results from the changes in solvent polarity. Thus, this means that the Fe-CO bond in  $[Fe(AzC18\alpha)(1,2-Me_2Im)(CO)]$  is shielded from the solvent polarity as observed in the pocket porphyrin complexes [11c]. Contrary to this, the increase of  $\nu(CO)$  for  $[Fe(AzC14\alpha)(1,2-Me_2Im)(CO)]$  suggests the unique conformation of the amide groups as revealed by the  $^1H$  NMR data. Comparing the  $\nu(CO)$  value of  $[Fe(AzP)(1,2-Me_2Im)(CO)]$ , the small  $\nu(CO)$  values of both  $[Fe(AzC14\alpha)(1,2-Me_2Im)(CO)]$  and  $[Fe(AzC18\alpha)(1,2-Me_2Im)(CO)]$  can be ascribed to four amide groups in the cavities, since the amide groups can

play the role of a primary solvation shell [25]. Although the change in  $\nu(\text{CO})$  between  $[\text{Fe}(\text{AzC14}\alpha)(1,2\text{-Me}_2\text{Im})(\text{CO})]$  and  $[\text{Fe}(\text{AzC18}\alpha)(1,2\text{-Me}_2\text{Im})(\text{CO})]$  was small, the change may be due to the steric repulsion on the bound CO molecule in  $[\text{Fe}(\text{AzC14}\alpha)(1,2\text{-Me}_2\text{Im})(\text{CO})]$ , since these two complexes have identical numbers of amide groups.

#### Effect of the Ruffling [26] of the Porphyrin Plane on O<sub>2</sub> or CO Binding

The porphyrin rings in 'strapped' porphyrins are considered to be ruffled by the strapping chains [27, 28]. Using 1,2-Me<sub>2</sub>Im as an axial base, the O<sub>2</sub> and CO affinities of iron(II) porphyrins decrease to approximately 1/40–1/50, compared with the case using 1-MeIm or 1,5-DCIm as an axial base [11d]. This is explained by the steric repulsion between the 2-methyl group and the porphyrin ring preventing movement of iron(II) toward the porphyrin plane upon O<sub>2</sub> or CO binding. Changing the axial base from 1,2-Me<sub>2</sub>Im to 1,5-DCIm, the O<sub>2</sub> and CO affinities of  $[\text{Fe}(\text{AzC14}\alpha)]$  decrease to approximately 1/200 and 1/120, respectively, as shown in Table 2. Thus, the larger changes in both O<sub>2</sub> and CO affinities suggest that the ruffling of the porphyrin ring in  $[\text{Fe}(\text{AzC14}\alpha)]$  is more severe than in flat porphyrins.

#### Solvent Effect on O<sub>2</sub> Binding

The solvent dependence of O<sub>2</sub> affinities for  $[\text{Fe}(\text{AzC14}\alpha)]$  was also examined at 0 °C with 1,2-Me<sub>2</sub>Im as an axial base. The  $P_{1/2}(\text{O}_2)$  values for  $[\text{Fe}(\text{AzC14}\alpha)]$  in mesitylene, toluene and *o*-dichlorobenzene were 260, 283 and 362 torr, respectively. The O<sub>2</sub> affinities for iron(II) porphyrins are known to increase with the increase of solvent polarity [11b, 14a, 14e]. Thus, the independence of the solvent polarity to the O<sub>2</sub> affinity suggests that the cavity in  $[\text{Fe}(\text{AzC14}\alpha)]$  is well shielded from solvent polarity.

#### Effect of Cavity Structure on O<sub>2</sub> or CO Binding

As seen in Table 2, the  $M$  value for  $[\text{Fe}(\text{AzP})(1,2\text{-Me}_2\text{Im})]$  is smaller than that for  $[\text{Fe}(\text{TpivPP})(1,2\text{-Me}_2\text{Im})]$  [5b] and is comparable to that for  $[\text{Fe}(\text{piv}_2\text{C9})(1,2\text{-Me}_2\text{Im})]$  [12]. The strapping group in  $[\text{Fe}(\text{AzP})]$  is the same as that in  $[\text{Fe}(\text{piv}_2\text{C9})]$ ; therefore, it is reasonable to expect that the C7-chain in  $[\text{Fe}(\text{AzP})]$  may cause certain effects such as a steric effect on O<sub>2</sub> or CO binding.

The O<sub>2</sub> affinity of  $[\text{Fe}(\text{AzC18}\alpha)]$  increases slightly, but the CO affinity decreases to 1/2, compared with the corresponding O<sub>2</sub> and CO affinities of  $[\text{Fe}(\text{AzP})]$ . The increased O<sub>2</sub> affinity for  $[\text{Fe}(\text{AzC18}\alpha)(1,2\text{-Me}_2\text{Im})]$  will be responsible for the presence of four amide groups which play the role of primary solvation shell [24a]. This suggestion is supported by the finding that  $\nu(\text{CO})$  of  $[\text{Fe}(\text{AzC18}\alpha)(1,2\text{-Me}_2\text{Im})(\text{CO})]$

is smaller than that of  $[\text{Fe}(\text{AzP})(1,2\text{-Me}_2\text{Im})(\text{CO})]$ . It is concluded that the amide groups of the C18-chain stabilize the Fe–O<sub>2</sub> bond not by H-bonding, since the amide H protons of the C7-chain form H-bonding in  $[\text{Fe}(\text{AzC18}\alpha)(1,2\text{-Me}_2\text{Im})(\text{O}_2)]$  as discussed in the <sup>1</sup>H NMR results. On the other hand, the reduced CO affinity of  $[\text{Fe}(\text{AzC18}\alpha)(1,2\text{-Me}_2\text{Im})]$  is partly responsible for the polar contribution of the amide groups. Nevertheless, it is difficult to explain the larger change in CO affinity than in O<sub>2</sub> affinity, because the effects of solvent polarity on the CO affinities are to no greater extent than in the O<sub>2</sub> affinities [12, 14e]. Thus, the reduced CO affinity must be mainly due to the steric effect of the C7-chain. Such a steric effect will be more evident in  $[\text{Fe}(\text{AzC14}\alpha)(1,2\text{-Me}_2\text{Im})]$ , in which the C7-chain is crushed by the steric interaction with the C14-chain as discussed in the <sup>1</sup>H NMR spectra.

The O<sub>2</sub> and CO affinities for  $[\text{Fe}(\text{AzC14}\alpha)(1,2\text{-Me}_2\text{Im})]$  decrease to approximately 1/140 and 1/660 compared with those of  $[\text{Fe}(\text{AzC18}\alpha)(1,2\text{-Me}_2\text{Im})]$ . Since both  $[\text{Fe}(\text{AzC18}\alpha)(1,2\text{-Me}_2\text{Im})]$  and  $[\text{Fe}(\text{AzC14}\alpha)(1,2\text{-Me}_2\text{Im})]$  have the four amide groups in their cavities, it is unreasonable to expect that the changes in both O<sub>2</sub> and CO affinities between two complexes are due to the polar effect of the amide groups in the cavities. Contrary to this, the difference between O<sub>2</sub> and CO affinities is well explained by the structural changes between the Fe–O<sub>2</sub> and Fe–CO moieties. The CO molecule binds linearly to the iron center [29], while O<sub>2</sub> molecule binds to the iron center in a bent fashion [30]. Thus, the Fe–CO bond has greater steric interaction with the strapped C7-chain than the Fe–O<sub>2</sub> bond, therefore a greater change in CO affinity than in O<sub>2</sub> is expected. In agreement with this, the change in the CO affinity for  $[\text{Fe}(\text{AzC14}\alpha)]$  is greater than in the O<sub>2</sub> affinity, compared with the CO and O<sub>2</sub> affinities for  $[\text{Fe}(\text{AzC18}\alpha)]$ . As a result, we postulate that the steric effect plays a major role in the discrimination between O<sub>2</sub> and CO bindings to  $[\text{Fe}(\text{AzC14}\alpha)]$ . There are no X-ray structural data at present and a recent report on a 'pocket' porphyrinatoiron(II) complex [31] also suggests that further work such as X-ray crystallographic study should be necessary to confirm our postulation.

Since the  $M$  value is equal to the ratio of the CO affinity to the O<sub>2</sub> affinity, the  $M$  value varies with both O<sub>2</sub> and CO affinities. Traylor *et al.* [14e] found a small  $M$  value ( $M = 14$ ) for 5,5-pyridine cyclophaneheme and they concluded that the small  $M$  value is mainly responsible for the increase in O<sub>2</sub> affinity by a polar effect. In contrast to this, we propose that the discrimination reaction between O<sub>2</sub> and CO to  $[\text{Fe}(\text{AzC14}\alpha)]$  is mainly responsible for the decrease in the CO affinity by a steric effect, as reported by Collman *et al.* [11d]. Comparing our study with the geometry of the active sites of de-

oxymyoglobin [32], oxymyoglobin [32] and carbonylmyoglobin [8], determined by X-ray analyses, there is reason to believe that the presence of imidazole in distal histidine increases the O<sub>2</sub> affinity by a polar effect, while on the other hand, it decreases the CO affinity by a steric effect. Therefore, our results may serve as useful information for the O<sub>2</sub> and CO discrimination reaction of hemoproteins.

## References

- (a) G. M. Giacometti, E. E. Di Iorio, E. Antonini, M. Brunori and K. H. Winterhalter, *Eur. J. Biochem.*, **75** (1977) 267; (b) G. M. Giacometti, M. Brunori, E. Antonini, E. E. Di Iorio and K. H. Winterhalter, *J. Biol. Chem.*, **255** (1980) 6160.
- P. W. Tucker, S. E. Phillips, M. F. Pertuz, R. Houtchens and W. S. Caughey, *Proc. Natl. Acad. Sci. U.S.A.*, **75** (1978) 1076.
- W. J. Wallace, J. A. Volpe, J. C. Maxwell, W. S. Caughey and S. Charache, *Biochem. Biophys. Res. Commun.*, **68** (1976) 1379.
- A. Szabo, *Proc. Natl. Acad. Sci. U.S.A.*, **75** (1978) 2108.
- E. J. Heidner, R. C. Ladner and M. F. Perutz, *J. Mol. Biol.*, **104** (1976) 707.
- J. Baldwin, *J. Mol. Biol.*, **136** (1980) 103.
- K. Moffat, J. F. Deatherage and D. W. Seybert, *Science*, **206** (1979) 1035.
- J. Kuriyan, S. Wilz, M. Karplus and G. A. Petsko, *J. Mol. Biol.*, **192** (1986) 133.
- (a) B. Luisi and K. Nagai, *Nature (London)*, **320** (1986) 555; (b) K. Nagai, B. Luisi, D. Shih, G. Miyazaki, K. Imai, C. Poyart, A. D. Young, L. Kwiatowsky, R. W. Noble, S. H. Lin and N. T. Yu, *Nature (London)*, **329** (1987) 858.
- D. H. Busch, L. L. Zimmer, J. J. Grzybowski, S. C. Olszanski, S. C. Jackels, R. C. Callahan and G. G. Christoph, *Proc. Natl. Acad. Sci. U.S.A.*, **78** (1984) 5919.
- (a) J. P. Collman, J. I. Brauman, T. R. Halbert and K. S. Suslick, *Proc. Natl. Acad. Sci. U.S.A.*, **73** (1976) 3333; (b) J. P. Collman, J. I. Brauman and K. M. Doxsee, *Proc. Natl. Acad. Sci. U.S.A.*, **76** (1979) 6035; (c) J. P. Collman, J. I. Brauman, T. J. Collins, B. L. Iverson, G. Lang, R. B. Pettman, J. L. Sessler and M. A. Walters, *J. Am. Chem. Soc.*, **105** (1983) 3038; (d) J. P. Collman, J. I. Brauman, B. L. Iverson, J. L. Sessler, R. M. Morris and Q. H. Gibson, *J. Am. Chem. Soc.*, **105** (1983) 3052.
- K. S. Suslick, M. M. Fox and T. J. Reinert, *J. Am. Chem. Soc.*, **106** (1984) 4522.
- M. Momenteau, B. Loock, C. Tetreau, D. Lavalette, A. Croisy, C. Schaeffer, C. Huel and J. M. Lhoste, *J. Chem. Soc., Perkin Trans. II*, (1987) 249.
- (a) T. G. Traylor and A. P. Berzini, *Proc. Natl. Acad. Sci. U.S.A.*, **77** (1980) 3171; (b) T. G. Traylor, M. J. Mitchell, S. Tsuchiya, D. H. Campbell, D. V. Stynes and N. Koga, *J. Am. Chem. Soc.*, **103** (1981) 5234; (c) T. G. Traylor, N. Koga, L. A. Deardurff, P. N. Swepston and J. A. Ibers, *J. Am. Chem. Soc.*, **106** (1984) 5132; (d) T. G. Traylor, S. Tsuchiya, D. Campbell, M. Mitchell, D. Stynes and N. Koga, *J. Am. Chem. Soc.*, **107** (1985) 604; (e) T. G. Traylor, N. Koga and L. A. Deardurff, *J. Am. Chem. Soc.*, **107** (1985) 6504.
- Y. Uemori, H. Miyakawa and E. Kyuno, *Inorg. Chem.*, **27** (1988) 377.
- M. Momenteau, J. Mispelter, B. Loock and E. Bisagni, *J. Chem. Soc., Perkin Trans. I*, (1983) 189.
- T. J. Beugelsdijk and R. S. Drago, *J. Am. Chem. Soc.*, **97** (1975) 6466.
- Y. Uemori and E. Kyuno, *Inorg. Chem.*, **28** (1989) 1690.
- Y. Uemori, A. Nakatsubo, H. Imai, S. Nakagawa and E. Kyuno, *Inorg. Chim. Acta*, **124** (1986) 153.
- J. W. Buchler, in K. M. Smith (ed.), *Porphyrin and Metalloporphyrins*, Elsevier, Amsterdam, 1975, pp. 157–231.
- J. C. Maxwell and W. S. Caughey, *Biochemistry*, **15** (1976) 388.
- R. J. Abraham, G. R. Bedford, D. McNeillie and B. Wright, *Org. Magn. Reson.*, **14** (1980) 418.
- M. Momenteau, W. R. Scheidt, C. W. Eigenbrot and C. A. Reed, *J. Am. Chem. Soc.*, **110** (1988) 1207.
- (a) D. Lavalette, C. Tetreau, J. Mispelter, M. Momenteau and J. M. Lhoste, *Eur. J. Biochem.*, **145** (1984) 555; (b) J. Mispelter, M. Momenteau, D. Lavalette and J. M. Lhoste, *J. Am. Chem. Soc.*, **105** (1983) 5165.
- D. Lexa, P. Maillard, M. Momenteau and J. M. Saveant, *J. Phys. Chem.*, **91** (1987) 1951.
- J. L. Hoard, in K. M. Smith (ed.), *Porphyrin and Metalloporphyrins*, Elsevier, Amsterdam, 1975, pp. 317–380.
- T. P. Wijesekera, J. B. Paine III and D. Dolphin, *J. Am. Chem. Soc.*, **105** (1983) 6747.
- U. Simonis, F. A. Walker, P. L. Lee, B. J. Hanquet, D. J. Meyerhoff and W. R. Scheidt, *J. Am. Chem. Soc.*, **109** (1987) 2659.
- S. M. Peng and J. A. Ibers, *J. Am. Chem. Soc.*, **98** (1976) 8032.
- G. B. Jameson, G. A. Rodley, W. T. Robinson, R. R. Gagne, C. A. Reed and J. P. Collman, *Inorg. Chem.*, **17** (1978) 850.
- K. Kim, J. Fettingner, J. L. Sessler, M. Cry, J. Hugdahl, J. P. Collman and J. A. Ibers, *J. Am. Chem. Soc.*, **111** (1989) 403.
- S. E. Phillips, *J. Mol. Biol.*, **142** (1980) 531.